Journal of Colloid and Interface Science 330 (2009) 67–72

Contents lists available at ScienceDirect

Journal of Colloid and Interface Science

www.elsevier.com/locate/jcis

Interactions of an anionic surfactant with poly(oxyalkylene) copolymers in aqueous solution

Antonios Kelarakis [a,*], Chiraphon Chaibundit [b], Marta J. Krysmann [c], Vasiliki Havredaki [a], Kyriakos Viras [a], Ian W. Hamley [c]

[a] National and Kapodistrian University of Athens, Department of Chemistry, Physical Chemistry Laboratory, Panepistimiopolis, 157 71 Athens, Greece
[b] Polymer Science Program, Faculty of Science, Prince of Songkla University, Hat Yai, Songkhla 90112, Thailand
[c] Department of Chemistry, University of Reading, PO BOX 224, Whiteknights, Reading RG6 6AD, UK

ARTICLE INFO

Article history:
Received 2 July 2008
Accepted 17 October 2008
Available online 22 October 2008

Keywords:
Anionic surfactant
Block copolymer
Complexation
Dynamic light scattering
Critical micelle concentration

ABSTRACT

The interactions of sodium dodecyl sulfate (SDS) with poly(ethylene oxide)/poly(alkylene oxide) (E/A) block copolymers are explored in this study. With respect to the specific compositional characteristics of the copolymer, introduction of SDS can induce fundamentally different effects to the self-assembly behavior of E/A copolymer solutions. In the case of the $E_{18}B_{10}$–SDS system (E = poly(ethylene oxide) and B = poly(butylene oxide)) development of large surfactant–polymer aggregates was observed. In the case of $B_{20}E_{610}$–SDS, $B_{12}E_{227}B_{12}$–SDS, $E_{40}B_{10}E_{40}$–SDS, $E_{19}P_{43}E_{19}$–SDS (P = poly(propylene oxide)), the formation of smaller particles compared to pure polymeric micelles points to micellar suppression induced by the ionic surfactant. This effect can be ascribed to a physical binding between the hydrophobic block of unassociated macromolecules and the non-polar tail of the surfactant. Analysis of critical micelle concentrations (cmc*) of polymer–surfactant aqueous solutions within the framework of regular solution theory for binary surfactants revealed negative deviations from ideal behavior for $E_{40}B_{10}E_{40}$–SDS and $E_{19}P_{43}E_{19}$–SDS, but positive deviations for $E_{18}B_{10}$–SDS. Ultrasonic studies performed for the $E_{19}P_{43}E_{19}$–SDS system enabled the identification of three distinct regions, corresponding to three main steps of the complexation; SDS absorption to the hydrophobic backbone of polymer, development of polymer–surfactant complexes and gradual breakdown of the mixed aggregates.

1. Introduction

The self-assembly properties of copolymers in selective solvents have been the subject of intense investigation in the last decades. Particular emphasis has been on the interactions between macromolecular amphiphiles and ionic surfactants. The polyelectrolyte nature of these polymeric-ionic complexes and the fact that multi component materials can enable better control of the aggregation properties compared to single surfactant systems make them promising candidates for a wide range of possible applications in colloid engineering such as templates for the development of nanoscale materials [1], drugs, coatings, pharmaceutical, petroleum and detergent formulations. In the field of nanotechnology, inclusion of ionic groups to the micellar core can effectively reverse their inherent non-polar nature, enabling their application as nanoreactors [1]. Furthermore, the advantage of using mixed surfactants solutions for the controlled fabrication of a variety of nanostructures has been recently demonstrated [2].

In this work, we report on the association properties of aqueous solutions that contain binary combinations of a single tailed surfactant, namely sodium dodecyl sulfate (SDS), together with poly(oxyalkylene) (E/A) copolymer. We consider diblock and triblock copolymers of poly(ethylene oxide)/poly(butylene oxide) (E/B) and poly(ethylene oxide)/poly(propylene oxide) (E/P). These materials represent a well-studied class of macromolecular surface-active agents that micellize in water, with the micellar core dominated by B or P blocks, while the E groups are extended in the solvent [3,4].

Much work on these systems has centered on the $E_mP_nE_m$ copolymers (subscripts denote number-average block lengths in chain units) available commercially from BASF (Pluronic) and Uniqema (Synperonic-PE). Detailed studies on the binding mechanism of $E_{97}P_{69}E_{97}$ (Pluronic F127) revealed four discrete stages on increasing SDS concentration; i.e. polymer micellization induced by SDS [5], formation of SDS–polymer complexes, collapse of complexes and complete inhibition of micellar growth [6–9]. Studies of poly(ethylene oxide) based copolymer–surfactant interactions have been extended to other copolymers having polystyrene (PSt) [10–15], polystyrene oxide (PStO) [16,17] and polybutadiene (PB)

* Corresponding author.
E-mail address: akelar@cc.uoa.gr (A. Kelarakis).

0021-9797/$ – see front matter
doi:10.1016/j.jcis.2008.10.045

[18–20] as the hydrophobic block. Calorimetry (mainly high sensitivity Differential Scanning Calorimetry and Isothermal Titration Calorimetry) has been employed to provide important insights to the binding mechanism, while critical information was obtained from surface tensiometry, static and dynamic light scattering and solution viscometry. A detailed list of the experimental methods used can be found in reference [21].

While the most common pattern of E/A–SDS interaction is that of destabilized polymeric micelles, there is increasing evidence in the literature that the presence of ionic surfactants can induce additional effects. It has been shown that addition of cetylpyridinium chloride (CPC) to E/PSt solutions can induce the formation of large aggregates [13], addition of SDS or DTAB in E/PB solution can cause the transformation of spherical micelles to large clusters or vesicles, the more so for polymers having lengthy hydrophobic units [19]. Large particles were also detected in E/PStO–SDS solutions [17], while in another E/PStO–SDS system non-monotonic decrease of hydrodynamic radius (r_h) upon increasing SDS loading was monitored [16]. Recently we have demonstrated a case of vesicle formation in E/B non-ionic surfactant aqueous solutions [22].

Within this framework, the aim of this study is to explore the possible patterns of E/A aggregation induced by ionic surfactant and examine the strength and the mechanism of the copolymer–surfactant interactions with respect to the nature of the hydrophobic repeating units and the polymer architecture. We attempt to provide a systematic and comparative study on anionic surfactant–E/A copolymer interactions, by considering five copolymers that have very different compositional characteristics and, therefore, very different micellar properties in water. A variety of experimental techniques were employed in this study; dynamic light scattering, surface tensiometry, conductimetry, volumetric and ultra sound velocity measurements.

2. Experimental

2.1. Materials

Copolymer $E_{40}B_{10}E_{40}$ was prepared by sequential anionic polymerization of 1,2-butylene oxide (BO) followed by ethylene oxide (EO). The difunctional initiator, 1,2-butane diol, was activated by potassium metal (molar ratio OH/K ≈ 10). Vacuum line and ampoule techniques were used to eliminate moisture. The preparation of copolymer $B_{20}E_{610}$ was by sequential anionic polymerization of BO followed by EO (we denote the polymers so produced as B_mE_n to signify the change in the copolymerization route), as described previously [23,24]. $B_{12}E_{227}B_{12}$ was prepared by oxyanionic polymerization of 1,2-butylene oxide initiated by poly(ethylene glycol), $M_n = 10000$ g/mol, that had been activated by mixing with KOH, as described in previous reports [25,26]. $E_{18}B_{10}$, $M_n = 1510$ g/mol was obtained from Dow Chemical Co. (code BM45-1600). $E_{19}P_{43}E_{19}$, $M_n = 4200$ g/mol was obtained from Uniqema (Synperonic PE/P84). For all polymers considered, gel permeation chromatography (GPC) was used to confirm narrow chain length distributions, and ^{13}C NMR spectroscopy was used to obtain absolute values of number-average molar mass. The molecular characteristics of copolymers used are summarized in Table 1.

Sodium dodecyl sulfate (SDS), purity >99%, was purchased from Acros Organics and was dried before used. Aqueous solutions in deionized and doubled distilled water were made by consecutive dilutions of a concentrated initial solution. All measurements were performed at 25 °C, with the exception of static light scattering that was performed in the temperature range 15–32 °C.

Table 1
Molecular and micellar characteristics of the copolymers.

Copolymer	M_n (g/mol)	M_w/M_n	cmc at 25 °C (mmol/dm^3)
$E_{18}B_{10}$	1510	1.04	0.05[a]
$B_{20}E_{620}$	28300	1.09	
$E_{19}P_{43}E_{19}$	4200	1.08	6.43[b]
$E_{40}B_{10}E_{40}$	4240	1.09	2.20[a]
$B_{12}E_{227}B_{12}$	11700	1.05	

Note. Estimated uncertainty: $M_n \pm 5\%$; $M_w/M_n \pm 0.01$, cmc ± 10%.
[a] Surface tension.
[b] Density and ultra sound velocity.

2.2. Methods

2.2.1. Dynamic light scattering (DLS)

Dynamic Light Scattering (DLS) measurements were carried out on well filtered solutions by means of an ALV/CGS-3 Compact Goniometer System with ALV/LSE-5003 correlator using vertically polarized incident light of wavelength $\lambda = 632.8$ nm. Measurements were performed at angle $\theta = 90°$ to the incident beam and data were collected three times for 30 s. The correlation functions (DLS) were analyzed by the constrained regularized CONTIN method [27] to obtain distributions of decay rates (Γ), hence distributions of apparent mutual diffusion coefficient $D_{app} = \Gamma/q^2$ [$q = (4\pi n/\lambda)\sin(\theta/2)$, where n is the refractive index of the solvent], and ultimately of apparent hydrodynamic radius of the particle via the Stokes–Einstein equation

$$r_h = kT/(6\pi\eta D_{app}), \quad (1)$$

where k is the Boltzmann constant and η is the viscosity of the solvent at temperature T.

2.2.2. Surface tension

Surface tension (γ) of aqueous solutions was measured by detachment of a platinum ring using a temperature-controlled (±0.2 °C) surface tensiometer (Kruss, Model K8600). The device was well protected from vibrations. The measurements were corrected with respect to the surface tension of the pure water (γ = 72.0 mN/m).

2.2.3. Conductivity

The conductivity (κ) of aqueous solutions was determined by a WTW microprocessor conductivity meter (Model LF539) using a Pt electrode. The accuracy of temperature control was ±0.1 °C. All measurements were corrected against the conductivity of the pure water ($\kappa = 0.6$ μS/cm).

2.2.4. Densities and ultrasonic velocities

Densities and ultrasonic velocities were measured by Anton Paar DMA 58 and DSA 48, respectively. In both devices, temperature control was maintained by internal Peltier systems, enabling an accuracy ±0.01 °C for DMA 58 and ±0.1 °C for DSA 48. The devices were calibrated against deionised and double distilled water and air. The density uncertainty was $\pm 1 \times 10^{-5}$ g/cm^3, and the ultrasonic velocity uncertainty was 10^{-2} m/s.

The apparent molar volumes ($V_{\phi,SDS}$) of aqueous copolymer solutions at a fixed polymer concentration were calculated via the equation:

$$V_{\phi,SDS} = (M_s/\rho) - 10^3(\rho - \rho_0)/(m_{SDS}\rho\rho_0), \quad (2)$$

where M_s is the molar mass and m_{SDS} is the molality (mol/kg) of SDS in the polymeric solution, ρ and ρ_0 are the densities of the ternary and binary solutions, respectively.

3. Results and discussion

3.1. Light scattering

Fig. 1 shows the intensity fraction distribution of the apparent hydrodynamic radius (r_h) of 1 wt% $E_{18}B_{10}$ aqueous solutions with various ionic surfactant molar fraction, a_{SDS} = moles of SDS/(moles of SDS + moles of polymer). Particles with r_h in the order of 100 nm are detected upon addition of SDS, compared to pure $E_{18}B_{10}$ micelles with $r_h = 7$ nm. The size of these super structures increases with surfactant loading up to $a_{SDS} = 0.8$ and start decomposing at higher surfactant loadings, indicating a saturation point of 4 SDS molecules per single polymer chain. We note that a similar molar fraction at saturation point has been determined for other related systems [14].

Although DLS plots are dominated by the diffusive motion of polymer–surfactant aggregates with radius in the order of 100 nm, the presence of two additional populations of micelles with smaller intrinsic volume has been demonstrated for a very similar system [22]. At the same time, Laser Scanning Confocal Microscopy (LSCM) revealed the development of larger vesicles [22] with sizes in the order of 500–1000 nm (such particles are filtered out in DLS experiments). Therefore, a multi component equilibrium involving vesicles of various sizes, polymer–SDS complexes and particles with primarily SDS content can be established for that system. Due to its low hydrophilic/hydrophobic length ratio, $E_{18}B_{10}$ can self-assembly in aqueous solution to form spheres, rods or vesicles, under certain conditions. For example upon heating spherical $E_{18}B_{10}$ micelles adopt a rod-like geometry due to reduced swelling of the EO block [28]. Dehydration of the corona can also be achieved by addition of salt, in which case vesicles can be formed [29]. Vesicle formation in mixed surfactant systems can be explained in terms of curvature free energy of the aggregates.

Polymer–surfactant super complexes of the same magnitude (r_h close to 100 nm) were also observed for $B_{12}E_{227}B_{12}$–SDS (Fig. 2) and $B_{20}E_{610}$–SDS systems (data not shown here). The apparent point of difference between Figs. 1 and 2 is the coexistence of smaller aggregates having r_h lower than that of neat polymer micelles. Based on the relative intensity of the two modes, it is clear that the population of larger particles increases with concentration

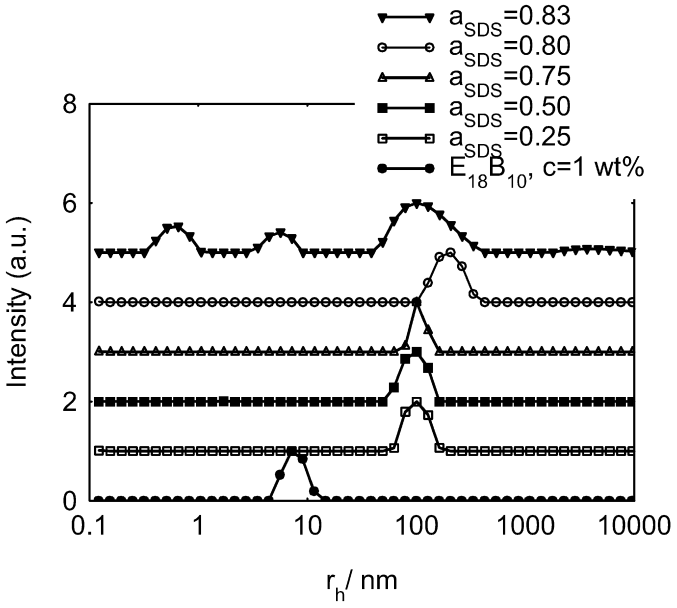

Fig. 1. Normalized intensity fraction distributions of apparent hydrodynamic radius (r_h) for aqueous solutions of $E_{18}B_{10}$–SDS complexes (copolymer concentration was kept constant 1 wt%) at 25 °C.

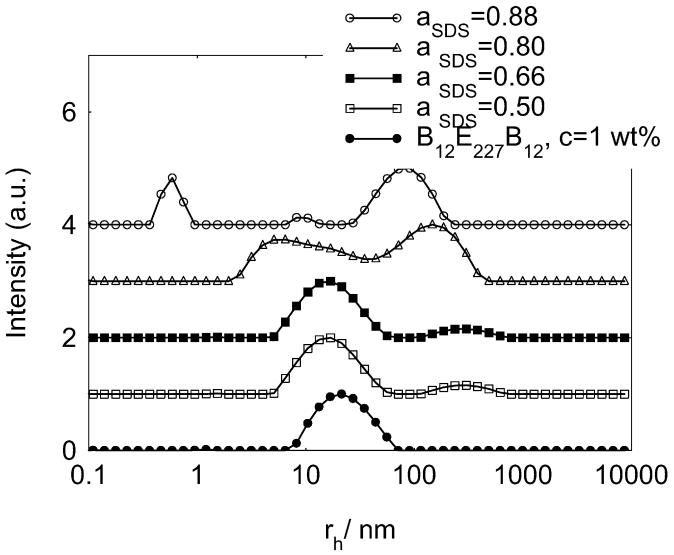

Fig. 2. Normalized intensity fraction distributions of apparent hydrodynamic radius (r_h) for aqueous solutions of $B_{12}E_{227}B_{12}$–SDS complexes (copolymer concentration was kept constant at 1 wt%) at 25 °C.

of added SDS. Moreover, the r_h value of both peaks monotonically decreases with increasing SDS concentration. From Fig. 2 a saturation point of 1 polymer to 8 SDS molecules can be concluded; i.e. the breakdown of aggregates takes place at increased molar fraction of SDS in the case of lengthy copolymers compared to shorter macromolecules (Fig. 1).

Multimodal distributions were observed for $E_{40}B_{10}E_{40}$–SDS and $E_{19}P_{43}E_{19}$–SDS systems as shown in Fig. 3. Increasing SDS content leads to smaller r_h values for both peaks and, at the same time, the signal of the higher r_h peak becomes stronger. The picture emerging from Figs. 2 and 3 is consistent with the behavior reported in the majority of surfactant-E/A studies [21]. The mechanism [7] proposed is based on surfactant absorption to hydrophobic backbone of the unassociated polymer, followed by the subsequent formation of surfactant–polymer complexes that progressively break down upon increased ionic loading due to increased repulsive interactions between the charged groups included in the complex structure.

With respect to compositional characteristics of the copolymers, different patterns of E/A–SDS interaction can be established. On one hand, the formation of particles having smaller size than the corresponding pure polymeric micelles points to micellar suppression induced by SDS, an effect that can be ascribed to a physical binding between the hydrophobic block of unassociated macromolecules and the non-polar tail of the surfactants. The formation of such complexes essentially reduces the concentration of the polymer unimers that are in dynamic equilibrium with polymer micelles destabilizing polymer micellization. On the other hand, detection of aggregates having higher intrinsic volume than the corresponding pure polymeric micelles can be assigned to the preferential formation of hydrogen bonds between water molecules and SDS, that create an unfavorable environment for polymeric chains, resulting in enhanced micellar size or promoting clustering.

3.2. Critical micelle concentration (cmc)

The critical micelle concentrations (cmc) of aqueous solutions of $E_{18}B_{10}$ and $E_{40}B_{10}E_{40}$ copolymers, as determined from surface tension measurements (Supporting material), are listed in Table 1. A value of cmc = 0.05 mmol/dm^3 was determined for $E_{18}B_{10}$, consistent with previously reported values 0.053 mmol/dm^3 at 20 °C,

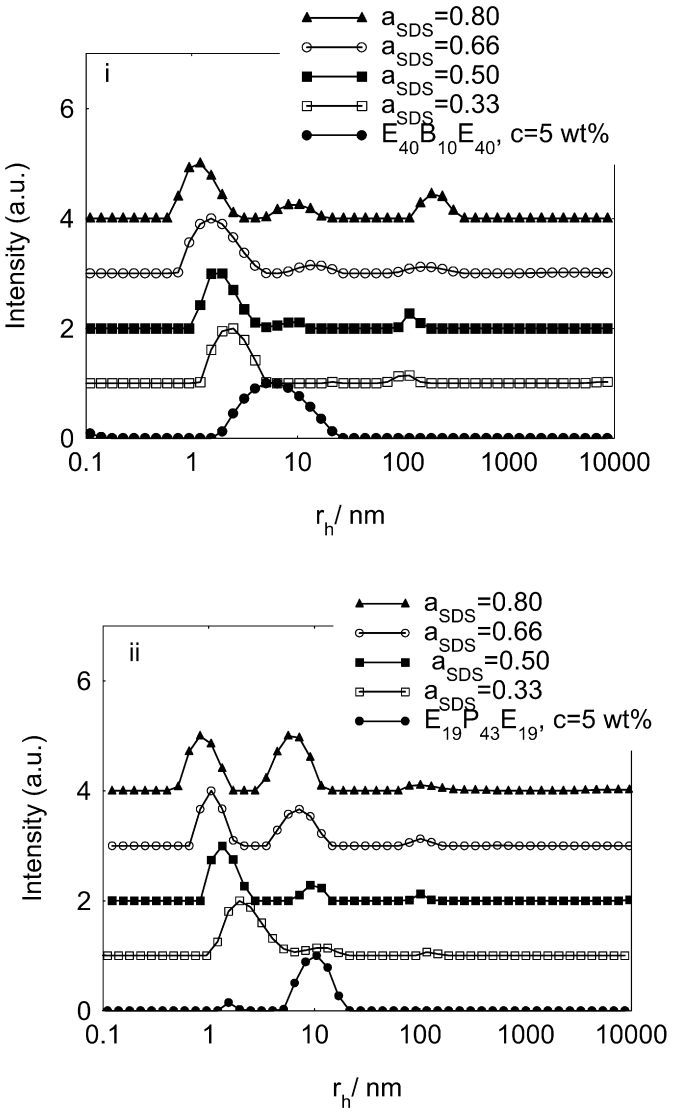

Fig. 3. Normalized intensity fraction distributions of apparent hydrodynamic radius (r_h) for aqueous solutions of (i) $E_{40}B_{10}E_{40}$–SDS and (ii) $E_{19}P_{43}E_{19}$–SDS complexes (copolymer concentration was kept constant at 5 wt%) at 25 °C.

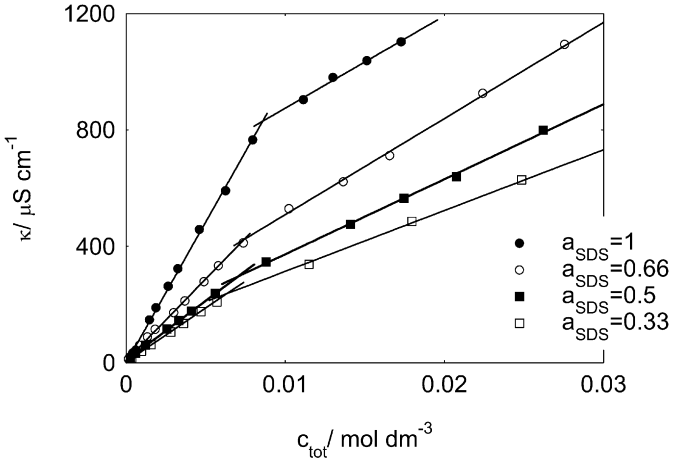

Fig. 4. Conductivity (κ) of $E_{18}B_{10}$–SDS aqueous solutions versus the total concentration of the surfactant (c_{tot}).

0.04 mmol/dm^3 at 30 °C [30]. Accordingly, cmc = 2.2 mmol/dm^3 was determined for $E_{40}B_{10}E_{40}$ that is also in close agreement with values reported for other triblock E/B copolymers, having comparable hydrophobic lengths [31,32]. We note the two orders of magnitude lower cmc of the diblock copolymer compared to the triblock one, an effect that points to the looping of the triblock molecules in the micelles given that each molecule is constrained by two block junctions in the core/fringe interface of the micelle, compared to only one constraint for the diblocks [3].

Due to the reduced hydrophobicity of the P unit compared to the B unit [3], the cmc of E/P copolymers can be determined with a vast variety of techniques; for example, in this work it was possible to determine cmc of $E_{19}P_{43}E_{19}$ at 25 °C based on data sets from ultrasonic velocity (u) and densimetric experiments (Supporting material). In particular, the cmc of $E_{19}P_{43}E_{19}$ could be identified as the break point of ultrasonic velocity or density as a function of copolymer concentration. The value of cmc = 6.43 mmol/dm^3, thus derived, falls within values previously reported for this copolymer [33].

In this report, the cmc of SDS was determined by conductimetry and found to be cmc = 8.3 mmol/dm^3 (Fig. 4, $a_{SDS} = 1$); e.g. as reported elsewhere [34]. Conductivity was also measured for the mixed systems $E_{18}B_{10}$–SDS, $E_{40}B_{10}E_{40}$–SDS, $E_{19}P_{43}E_{19}$–SDS at a variety of surfactant molar fractions. In all cases the data sets could be satisfactory fitted with two straight lines, whose intersection was taken as the critical micelle concentration of the mixed system cmc*. A representative conductivity profile is shown in Fig. 4 for $E_{18}B_{10}$–SDS system. Fig. 5 gathers cmc* values determined from such conductivity profiles for the three systems studied; $E_{18}B_{10}$–SDS (Fig. 5i), $E_{40}B_{10}E_{40}$–SDS (Fig. 5ii), $E_{19}P_{43}E_{19}$–SDS (Fig. 5iii).

Several thermodynamic models have been developed in order to describe surfactant–surfactant interactions. Within the framework of regular solution theory (RST) the critical micelle concentration (cmc*) of binary surfactant mixtures follows the relationship [35]:

$$\mathrm{cmc}^* = \left[\sum \alpha_i / f_i(\mathrm{cmc}_i)\right]^{-1}, \tag{3}$$

where cmc_i represents the cmc values of the pure components, α_i the molar fraction of the respective surfactant and f_i are the activity coefficients of the component i within the mixed micelle. In a binary system, the f_i values are related with the interaction parameter β:

$$f = \exp\left[\beta(1-x_1)^2\right], \tag{4}$$

$$f_2 = \left[\exp \beta x_1^2\right], \tag{5}$$

where x_1 is the mole fraction of the surfactant 1 in the mixed micelle and can be calculated from the equation:

$$x_1^2 \ln(\alpha_i \mathrm{cmc}^*/x_1 \mathrm{cmc}_1) = (1-x_1^2)\ln\left[(1-\alpha_i)\mathrm{cmc}^*/(1-x_1)\mathrm{cmc}_2\right]. \tag{6}$$

This analytical approach for non ionic–ionic surfactants has been applied to both theoretical [36] and experimental [37] investigations including studies for EPE–ionic surfactant systems [38,39].

For ideal mixing (Clint model [40]) $\beta = 0$, while non zero values are assumed to arise from specific surfactant–surfactant interactions. A negative deviation from ideal behavior, such as that observed in Figs. 5i and 5ii, can be assigned to a certain attraction between the two different surfactant molecules. For $E_{40}B_{10}E_{40}$–SDS and $E_{19}P_{43}E_{19}$–SDS $\beta = -2.7$ and $\beta = -2.3$, respectively. These values can be compared with $\beta = -4.5$ (from electromotive force measurements) and $\beta = -7.4$ (from surface tension and ITC measurements) for $E_{97}P_{69}E_{97}$ (F127)–SDS at 25 °C [38] and $-2.6 < \beta < -1.0$ for Triton X100 with different anionic surfactants [37].

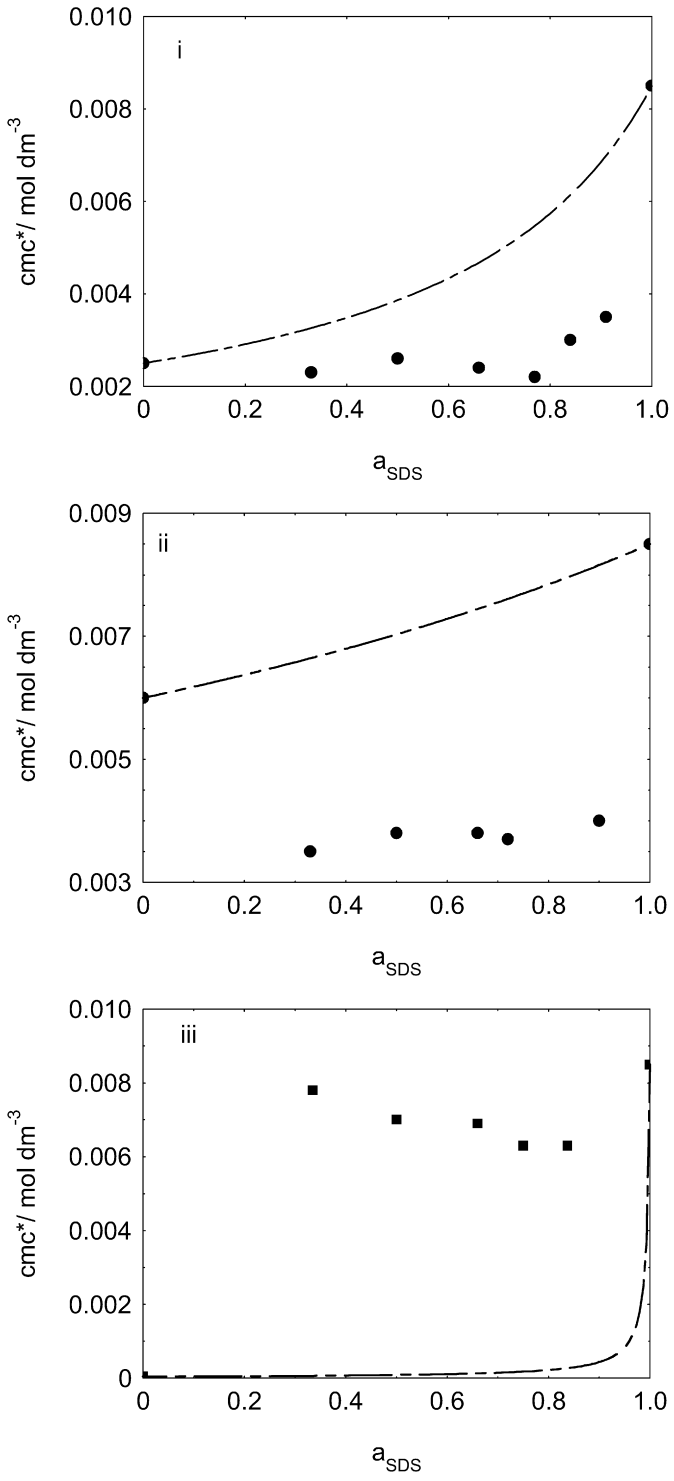

Fig. 5. Experimental (markers) and predicted (lines) cmc* (expressed in mol/dm^3, corresponding to the concentration of both polymer and SDS) of (i) $E_{40}B_{10}E_{40}$–SDS, (ii) $E_{19}P_{43}E_{19}$–SDS and (iii) $E_{18}B_{10}$–SDS system as a function of the mole fraction of SDS.

On the other hand, $E_{18}B_{10}$–SDS exhibits fundamentally different behavior; cmc* values obtained experimentally are much higher than the corresponding cmc* calculated from ideal mixing, as shown in Fig. 5iii. Positive deviations from ideal mixing have been attributed to antagonistic effects between the two different surfactants. In the case of nonionic–ionic surfactants only negative deviations have been theoretically predicted [41] and experimentally observed. The unique behavior observed for $E_{18}B_{10}$–SDS is

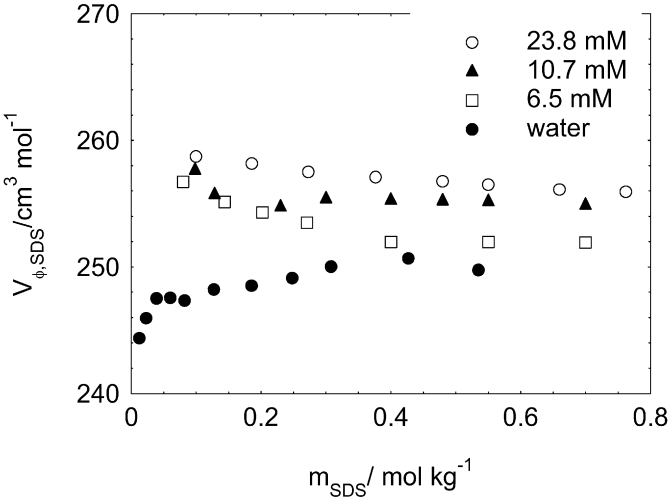

Fig. 6. Apparent molar volumes of SDS ($V_{\phi,SDS}$) versus SDS molality in water (filled circles) and in aqueous solutions of $E_{19}P_{43}E_{19}$ 6.5 mM (squares), 10.7 mM (triangles) and 23.8 mM (open circles).

directly related to the vesicular geometry of the resultant polymer–surfactant complexes. In other words, the dramatic effects induced by SDS in $E_{18}B_{10}$ micellar solutions cannot be efficiently considered within the framework of RST for ideal mixtures, in strong contrast with the other E/A–ionic surfactant systems studied here and in previous reports.

3.3. Volumetric and ultrasonic studies in $E_{19}P_{43}E_{19}$–SDS

The variation of apparent molar volumes of SDS ($V_{\phi,SDS}$) versus SDS molality in water and in aqueous solutions containing several fixed amounts of $E_{19}P_{43}E_{19}$ is presented in Fig. 6. Given that cmc of $E_{19}P_{43}E_{19}$ is 6.4 mM (Table 1), it can be concluded that the polymer is in its monomeric form for the lowest concentration (6.5 mM), partially micellized for the intermediate concentration (10.7 mM) and almost fully micellized for the highest concentration (23.8 mM). Nevertheless, the three curves of the mixed systems exhibit the same trends, regardless of the state of dispersion (monomeric or micellar) of the initial ($a_{SDS} = 0$) solutions.

It can be clearly seen that at low SDS content $V_{\phi,SDS}$ is significantly higher in ternary systems, while the difference in $V_{\phi,SDS}$ between ternary and binary systems progressively diminishes at higher SDS concentrations. It should be noted that $V_{\phi,SDS}$ in $E_{13}P_{30}E_{13}$ (L64) solutions was shown to exhibit very similar behavior [42] with that reported here. It is well established that the composition dependence of the apparent molar volume of a solute in a ternary system reflects the solute–solute, solvent–solute and solvent–solvent interactions. In the particular case studied here, the pronounced increase of $V_{\phi,SDS}$ is consistent with the evolution of polymer–SDS complexes. It is, therefore, evident that both monomers and micelles of $E_{19}P_{43}E_{19}$ spontaneously bind to SDS molecules, giving rise to enhanced $V_{\phi,SDS}$. At higher SDS concentration, the copolymer chains get saturated with SDS molecules and $V_{\phi,SDS}$ in the ternary system approaches that in pure water.

In Fig. 7, the ultrasound velocity (u) of aqueous solution of $E_{19}P_{43}E_{19}$ is plotted as a function of added SDS. The three plots shown in Fig. 7 share the same common features; upon SDS addition they show an initial decrease, followed by an increase, a plateau zone and finally a second drop region. When a small amount of SDS is initially added u decreases sharply, indicating the formation of polymer–surfactant aggregates with less compact structure compared to the pure polymer micelles or polymer monomers. For all three plots presented in Fig. 7 a local minimum

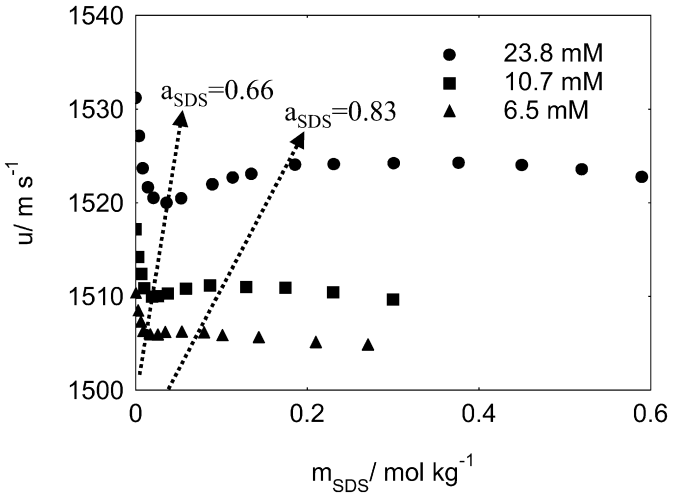

Fig. 7. Ultrasonic velocity (u) versus concentration of added SDS in solutions containing $E_{19}P_{43}E_{19}$ 6.5 mM (triangles), 10.7 mM (squares) and 23.8 mM (circles). Dashed lines are guide to eye and correspond to $a_{SDS} = 0.66$ and $a_{SDS} = 0.83$.

can be observed that falls close to $a_{SDS} = 0.66$. Further addition of SDS results in increased u, tending to a plateau region in which the ultrasound velocity remains essentially constant. This common feature of the three curves reflects the presence of two competing effects; the progressively increased particle density on one hand, that is responsible for the increase of u, and the lower association numbers of the mixed aggregates that tends to reduce u values on the other hand. There is solid experimental evidence for the presence of those two parallel effects on the basis of SANS plots, performed for the $E_{97}P_{69}E_{97}$–SDS system [7]. Excess addition of ionic component leads to a gradual collapse of complexes due to the strong electrostatic repulsion between the headgroups of SDS. Therefore, u values drop tending to the lower value of pure SDS micelles (for example for 0.4 m SDS in water, ultrasound velocity was measured $u = 1497\ \mathrm{m\,s^{-1}}$). This final drop of u versus m plots starts at $a_{SDS} = 0.83$ for all three polymer concentrations considered. The three different regions (defined by the two dashed lines) shown in Fig. 7 graphically depict the behavior presented above.

4. Conclusions

In this work we report a systematic and comparative study on the interaction of an anionic surfactant with a series of E/A block copolymers. Introduction of SDS to aqueous solutions of $E_{18}B_{10}$ induces a drastic effect on polymer curvature, giving rise to large vesicles. We demonstrate here that the cmc* of the vesicular aggregates show positive deviations from the ideal mixing of mixed surfactants, as opposed to the interaction pattern established for other SDS–E/A systems that they do not form vesicles. In addition, large particles (though as a minor component) were also detected in solutions of $B_{20}E_{610}$–SDS and $B_{12}E_{227}B_{12}$–SDS systems, indicating micellar clustering. At the same time, in the case of $B_{20}E_{610}$–SDS, $B_{12}E_{227}B_{12}$–SDS, $E_{40}B_{10}E_{40}$–SDS, $E_{19}P_{43}E_{19}$–SDS the development of particles having lower intrinsic volumes compared to pure polymeric micelles points to micellar suppression induced by the ionic surfactant. This effect can be traced back to the absorption of surfactant tails to the poly(alkylene oxide) chains. Electrostatic repulsions between charged groups lead to destabilization of mixed micelles compare to the pure polymeric micelles. Lastly, we demonstrate that measurements of ultra sound velocity can provide insightful information for the dynamics of those complex systems.

Acknowledgments

A.K. was supported by the Greek Ministry of Development-General Secretariat of Research and Technology within the 04EP36 (ENTER) research project.

Supporting material

The online version of this article contains additional supplementary material.

Please visit DOI: 10.1016/j.jcis.2008.10.045.

References

[1] L.M. Bronstein, D.M. Chernyshov, G.I. Timofeeva, L.V. Dubrovina, P.M. Valetsky, E.S. Obolonkova, A.R. Khokhlov, Langmuir 16 (2000) 3626.
[2] N. Zhao, Y. Wei, N. Sun, Q. Chen, J. Bai, L. Zhou, Y. Qin, M. Li, L. Qi, Langmuir 24 (2008) 991.
[3] C. Booth, D. Attwood, Macromol. Rapid Commun. 21 (2000) 501.
[4] C. Booth, D. Attwood, C. Price, Phys. Chem. Chem. Phys. 8 (2006) 3612.
[5] Y. Li, R. Xu, S. Couderc, D.M. Bloor, E. Wyn-Jones, J.F. Holzwarth, Langmuir 17 (2001) 183.
[6] E. Hecht, H. Hoffmann, Langmuir 10 (1994) 86.
[7] E. Hecht, K. Mortensen, M. Gradzielski, H. Hoffmann, J. Phys. Chem. 99 (1995) 4866.
[8] E. Hecht, H. Hoffmann, Colloids Surf. 96 (1995) 181.
[9] S.M. Ghoreishi, G.A. Fox, D.M. Bloor, J.F. Holzwarth, E. Wyn-Jones, Langmuir 15 (1999) 5474.
[10] K. Nakamura, R. Endo, T. Masatani, J. Polym. Sci. Polym. Phys. Ed. 15 (1977) 2087.
[11] P. Bahadur, N.V. Sastry, Y.K. Rao, G. Riess, Colloids Surf. 29 (1988) 343.
[12] K. Contractor, C. Patel, P. Bahadur, J. Macromol. Sci. Pure Appl. Chem. A 34 (1997) 2497.
[13] L.M. Bronstein, D.M. Chernyshov, G.I. Timofeeva, L.V. Dubrovina, P.M. Valetsky, E.S. Obolonkova, A.R. Khokhlov, Langmuir 16 (2000) 3626.
[14] L.M. Bronstein, D.M. Chernyshov, G.I. Timofeeva, L.V. Dubrovina, P.M. Valetsky, A.R. Khokhlov, J. Colloid Interface Sci. 230 (2000) 140.
[15] L.M. Bronstein, D.M. Chernyshov, E. Vorontsov, G.I. Timofeeva, L.V. Dubrovina, P.M. Valetsky, S. Kazakov, A.R. Khokhlov, J. Phys. Chem. 105 (2001) 9077.
[16] E. Castro, P. Taboada, V. Mosquera, J. Phys. Chem. B 109 (2005) 5593.
[17] P. Taboada, E. Castro, V. Mosquera, J. Phys. Chem. B 109 (2005) 23760.
[18] Y. Zheng, H.T. Davis, Langmuir 16 (2000) 6453.
[19] S. Pispas, N. Hadjichristidis, Langmuir 19 (2003) 48.
[20] H. Egger, A. Nordskog, P. Lang, A. Brandt, Macromol. Symp. 162 (2000) 291.
[21] N.V. Sastry, H. Hoffmann, Colloids Surf. A Physicochem. Eng. Aspects 250 (2004) 247, and references therein.
[22] A. Kelarakis, V. Castelletto, M.J. Krysmann, V. Havredaki, K. Viras, I.W. Hamley, Langmuir 24 (2008) 3767.
[23] A. Kelarakis, V. Havredaki, K. Viras, W. Mingvanish, F. Heatley, C. Booth, S.-M. Mai, J. Phys. Chem. B 105 (2001) 7384.
[24] A. Kelarakis, J.J. Crassous, M. Ballauff, Z. Yang, C. Booth, Langmuir 22 (2006) 6814.
[25] A. Kelarakis, X.-T. Ming, X.-F. Yuan, C. Booth, Langmuir 20 (2004) 2036.
[26] A. Kelarakis, X.-F. Yuan, S.-M. Mai, Y.-W. Yang, C. Booth, Phys. Chem. Chem. Phys. 5 (2003) 2628.
[27] S.W. Provencher, Makromol. Chem. 180 (1979) 201.
[28] I.W. Hamley, J.S. Pederson, C. Booth, V.M. Nace, Langmuir 17 (2001) 6386.
[29] J.K. Harris, G.D. Rose, M.L. Bruening, Langmuir 18 (2002) 5337.
[30] A. Kelarakis, V. Havredaki, C. Booth, V.M. Nace, Macromolecules 35 (2002) 5591.
[31] G.-E. Yu, Y.-W. Yang, Z. Yang, D. Atwood, C. Booth, V.M. Nace, Langmuir 12 (1996) 3404.
[32] G.-E. Yu, H. Li, C. Price, C. Booth, Langmuir 18 (2002) 7756.
[33] P. Alexandridis, J.F. Holzwarth, T.A. Hatton, Macromolecules 27 (1994) 2414.
[34] M.S. Bakshi, J. Chem. Soc. Faraday Trans. 89 (1993) 4323.
[35] P.M. Holland, Adv. Colloid Interface Sci. 26 (1986) 111.
[36] I. Reif, P. Somasundaran, Langmuir 15 (1999) 3411.
[37] C. Ruiz Carnero, J. Aquiar, Langmuir 16 (2000) 7946.
[38] T. Thurn, S. Couderc, J. Sidhu, D.M. Bloor, J. Penfold, J.F. Holzwarth, E. Wyn-Jones, Langmuir 18 (2002) 9267.
[39] M.S. Bakshi, S. Sachar, Colloids Surf. A Physicochem. Eng. Aspects 276 (2006) 146.
[40] J.H. Clint, J. Chem. Soc. Faraday Trans. 71 (1975) 1372.
[41] M. Bergstrom, J.C. Eriksson, Langmuir 16 (2000) 7173.
[42] S. Senkov, A.H. Roux, G. Roux-Desgranges, Phys. Chem. Chem. Phys. 6 (2004) 822.